



저작자표시-비영리-변경금지 2.0 대한민국

이용자는 아래의 조건을 따르는 경우에 한하여 자유롭게

- 이 저작물을 복제, 배포, 전송, 전시, 공연 및 방송할 수 있습니다.

다음과 같은 조건을 따라야 합니다:



저작자표시. 귀하는 원저작자를 표시하여야 합니다.



비영리. 귀하는 이 저작물을 영리 목적으로 이용할 수 없습니다.



변경금지. 귀하는 이 저작물을 개작, 변형 또는 가공할 수 없습니다.

- 귀하는, 이 저작물의 재이용이나 배포의 경우, 이 저작물에 적용된 이용허락조건을 명확하게 나타내어야 합니다.
- 저작권자로부터 별도의 허가를 받으면 이러한 조건들은 적용되지 않습니다.

저작권법에 따른 이용자의 권리는 위의 내용에 의하여 영향을 받지 않습니다.

이것은 [이용허락규약\(Legal Code\)](#)을 이해하기 쉽게 요약한 것입니다.

[Disclaimer](#)

Designing anti-HER2 multi-paratopic nanobody for bending-induced inactivation

Do Hyeon Kim

Department of Medical Science

The Graduate School, Yonsei University

Designing anti-HER2 multi-paratopic nanobody for bending-induced inactivation


Directed by Professor Joo Young Kim

The Master's Thesis
submitted to the Department of Medical Science,
the Graduate School of Yonsei University
in partial fulfillment of the requirements for the degree of
Master of Medical Science

Do Hyeon Kim

December 2023

This certifies that the Master's Thesis of
Do Hyeon Kim is approved.



Thesis Supervisor: Joo Young Kim

Thesis Committee Member#1 : Minkyu Jung

Thesis Committee Member#2: Won-Kyu Lee

The Graduate School
Yonsei University

December 2023

ACKNOWLEDGEMENTS

First and foremost, I would like to express my profound gratitude to Professor Joo Young Kim for her invaluable guidance and unwavering support throughout my entire journey in graduate school. The two years I spent in Professor Kim's laboratory were genuinely enriching, igniting my passion and shaping my future career path. It is a great honor for me to have completed my master's degree at Yonsei University under Professor Kim's supervision.

I also wish to extend my heartfelt appreciation to Professor Minkyu Jung and Dr. Won-kyu Lee for their significant contributions as members of my thesis committee. Their abundant advice and constructive feedback played a pivotal role in my development as a seasoned scientist.

Dr. Dong Hyuk Lee, whom I consider one of the most admirable individuals I've ever encountered in my lifetime, served as an exceptional mentor and colleague, providing me with extensive guidance and instruction. I would like to convey my immense appreciation to him as well.

I must express my gratitude to A Yeon, Yerim, Geun Ah, and Beom Jun, Jin Kyung for their camaraderie, shared insights, and invaluable teamwork in our laboratory. Your contributions were truly exceptional.

Lastly, but certainly not least, I extend my deepest gratitude to my parents for their boundless love and unwavering support throughout my entire life. I love you dearly

<TABLE OF CONTENTS>

ABSTRACT	v
I. INTRODUCTION	1
II. MATERIALS AND METHODS	4
1. Cells	4
2. Sequences of used primers	4
3. Ribosomal display	4
4. Reverse transcription	5
5. qPCR	6
6. Making Electro component SS320 cell	6
7. Electroporation	6
8. Production and purification of the phage	7
9. Phage display	7
10. Cell binding assay using output phages from each Phage Display	9
11. ELISA	9
12. Production and purification of the nanobodies	10
13. Cloning HER2-EGFP	10
14. HER2 Domain expression	11
15. <i>In-silico</i> nanobody prediction	11
16. <i>In-silico</i> HER2-nanobody Docking prediction	11
17. HER2 crystal structure analysis	11
18. Making multi-paratopic nanobody	12
19. Binding assay	12
20. Amin conjugation pH sensing dye to antibody	12
21. Checking endocytosis	13
22. Confocal image	13

23. Cell viability	13
24. Lentivirus production	13
25. Generation of GFP-dCas9-SNU-1 cell	14
26. Generation of HER2 overexpression cell	14
27. Cloning of CRISPRi ERBB2 sgRNA	14
28. HER2 Knockdown using CRSPRi system	14
29. Bio-layer interferometry (BLI)	15
30. Epitope binning using BLI	15
31. Cloning of multi-paratopic nanobody	15
32. Expression of multi-paratopic nanobody	16
33. Antibody purification	16
34. Statistical analysis	17
III. RESULTS	18
1. Low effect of Trastuzumab in low HER2 gastric cancer	18
2. Screening of anti-HER2 nanobody	21
3. Purification and binding of nanobody	24
4. The distinction of nanobodies binding each domain	27
5. Design of multi-paratopic nanobody using <i>in-silico</i>	31
6. Effect of multi-paratopic nanobody	34
7. Effect of Fc-fusion multi-paratopic nanobody	37
IV. DISCUSSION	40
V. CONCLUSION	42
REFERENCES	43
APPENDICES	47

ABSTRACT (IN KOREAN)	48
-----------------------------	----

LIST OF FIGURES

Figure 1. HER2 expression & endocytosis in gastric cancer	19
Figure 2. Generation of HER2 knockdown & overexpression cell line	20
Figure 3. Screening of synthetic nanobody against the HER2	22
Figure 4. Purification and assesment cell binding	25
Figure 5. Distinguish of nanobodies binding domain using <i>in-vitro</i> and <i>in-silico</i>	28
Figure 6. <i>In-silico</i> HER2 structure analysis and design of multi - paratopic nanobody	32
Figure 7. Purification and function of multi-paratopic nanobody	35
Figure 8. Purification and function of FC-fusion multi-paratopic nanobody	38

LIST OF TABLES

Table 1. Result of <i>in-silico</i> docking score	47
Table 2. Result of binding affinity	47

ABSTRACT

Designing anti-HER2 multi-paratopic nanobody for bending-induced inactivation

Do Hyeon Kim

*Department of Medical Science
The Graduate School, Yonsei University*

(Directed by Professor Joo Young Kim)

Trastuzumab is a monoclonal antibody that targets HER2 receptors and is effectively used to inhibit cell growth and induce cell death. In addition, T-DM1, antibody-drug binding (ADC) of trastuzumab, effectively delivers drugs into cells by endocytosis then induces apoptosis. However, this effect can be limited in cancer cells with low HER2 expression. In a recent study, it was reported that the domain II portion of HER2 plays a role in inhibiting heterodimeric intracellular influx. In this study, we discovered nanobodies that bind to multiple domains of HER2 and designed multiple paratope nanobodies that not only have improved binding power but also induce inactivation through structural changes in HER2 domain II. After discovering multiple nanobodies through screening of a synthetic nanobody library with 10^{12} diversity, we predicted the sites that bind to HER2 by *in-silico* method and identified that they bind to actual fragmented HER2 proteins by biochemical methods to select nanobodies that bind to different domains I, II, and III. Among the multi-bond forms configured with the three nanobodies, we observed that the configuration with a short, flexible linker in the binding order of domain I, III, and II was effective. In their Fc forms, the order of I, II, and III with higher binding affinity than I, III, and II orders demonstrated effectiveness. In conclusion, this study provides a novel inactivation strategy for HER2 by inducing structural changes in HER2 itself, as well as increasing binding affinity for HER2 in malignant tumors such as gastric cancer.

Key words: HER2, multi-paratopic, endocytosis, nanobody, trastuzumab, *in-silico* method

Designing anti-HER2 multi-paratopic nanobody for bending-induced inactivation

Kim Do Hyeon

*Department of Medical Science
The Graduate School, Yonsei University*

(Directed by Professor Joo Young Kim)

I. INTRODUCTION

Gastric Cancer (GC) is a disease that places a great burden on national health due to its high incidence rate among all malignancies¹. Within the context of GC, the overexpression of Human epidermal growth factor receptor 2 (HER2) is a prevalent occurrence, with estimates suggesting it is observed in approximately 10% to 30% of gastric cancer cases^{2, 3, 4}. Consequently, HER2 has emerged as a critical biomarker for the development of diagnostic and therapeutic approaches utilizing antibodies in the management of gastric cancer^{2, 5}.

Trastuzumab, a recombinant humanized monoclonal antibody, has demonstrated its effectiveness in inhibiting HER2 signaling pathways, thereby suppressing cell proliferation⁶. Additionally, it exerts its therapeutic action through various mechanisms, including the promotion of antibody-dependent cell-mediated cytotoxicity (ADCC)⁷ and the induction of endocytosis and subsequent degradation of HER2 by specifically binding to the IV domain of the HER2 receptor^{8, 9}.

However, a significant challenge arises in the context of gastric cancers that express low levels of HER2, as these cases are often associated with a poor prognosis and tend to exhibit resistance to trastuzumab therapy¹⁰. To address this issue, a combination therapy approach has been employed, where trastuzumab is used alongside chemotherapy, with the

aim of enhancing treatment efficacy⁴. Another notable development is the creation of T-DM1, which is a conjugate of trastuzumab and emtansine. T-DM1 operates by inducing cell cycle arrest and apoptosis in HER2-positive cancer cells¹¹.

Despite these advances, there remain limitations in achieving satisfactory therapeutic outcomes when dealing with low HER2 expression in gastric cancer. Consequently, numerous research studies are actively exploring innovative strategies to improve drug delivery and treatment efficacy in cases where HER2 expression is low¹².

Indeed, recent research findings have shed light on the intriguing phenomenon of antibody-induced rapid internalization¹³. This discovery has sparked considerable interest in the field of HER2-targeted therapies. Notably, antibodies that simultaneously target both the II domain and the IV domain of HER2 have been successfully developed. These dual-targeting antibodies exhibit a remarkable capability for inducing rapid internalization compared to the treatment with trastuzumab alone^{14,15}. These compelling findings underscore the importance of diversifying antibody development efforts to target distinct epitopes of HER2.

Besides, the emergence of anti-HER2 nanobodies represents another exciting development in the quest to combat HER2-related tumor growth. These nanobodies are designed to bind to two different paratopes of HER2, effectively engaging with multiple regions of the receptor^{16, 17}. This multifaceted binding strategy holds great promise in inhibiting tumor growth and opens up new avenues for the development of therapies that can effectively counter HER2-overexpressing tumors.

As well as, it's worth noting that when the HER2-EGFR complex was formed after binding to epidermal growth factor (EGF), a remarkable phenomenon occurs their endocytosis is inhibited due to the specific conformation of the HER2 domain II^{19, 20, 21}. Unlike other receptor complexes, in this case, the HER2 remains in an unbent form because of domain II²⁰. This unique configuration induces the formation of a stable heterodimer complex, allowing the continuous stimulation of tyrosine kinase signaling pathways while concurrently blocking the endocytosis signals that would normally lead to the

internalization and degradation of the receptor complex. This intricate interplay between molecular structures and signaling pathways highlights the complex regulatory mechanisms governing cellular responses to growth factors like EGF²⁰. Additionally, an interesting observation emerges when a specific mutation occurs within HER2, specifically at the 310-serine residue, resulting in its conversion to phenylalanine. In this altered state, HER2 exhibits a heightened propensity to form robust complexes with HER3 and EGFR²⁰.

Building on this, the strategy to induce a conformational change in HER2 for enhanced endocytosis involves identifying binders targeting each domain. Computational technology plays a crucial role in this process, particularly through *in-silico* -based nanobody structure optimization and design using protein-protein docking methods^{22, 23}. The prediction of conformational domains relies on a variety of computational techniques, including mono-protein structure modeling with tools like AlphaFold 2, protein-protein docking simulations, molecular dynamic simulations, and the continuous advancements in machine learning approaches^{24, 25, 26}.

In this study, we discover nanobodies that bind to each domain of HER2. And by producing these multi-binding molecules using *in-silico* method, we intend to increase endocytosis by morphologic change in addition to enhancing binding force by multiple bonds. This can suggest a method for targeting HER2 as well as for increasing the HER2 inactivation by inducing the bending of HER2 structure.

II. MATERIALS AND METHODS

1. Cell

SNU-1, NCI-N87, MKN-7, gastric cancer cells, were cultured with RPMI 1640 (WELGENE, LM011-60) containing 10% FBS (WELGENE, S 101-01) and 1% penicillin/streptomycin (P/S; WELGENE, LS 202-02). SKBR3, breast cancer cell, HEK293T were cultured with DMEM (WELGENE, LM001-05) containing 10% FBS (WELGENE, S 101-01) and 1% penicillin/streptomycin. All cell lines were incubated at 37 °C and 5% CO₂ incubator.

2. Sequences of used primers

The primer information utilized in this study to generate synthetic nanobodies was obtained from the pertinent paper dedicated to the subject¹⁸. The Long FX forward (ATA TGC TCT TCT AGT CAA GTC CAG CTG GTG GAA TCG), the Long FX reverse (TAT AGC TCT TCA TGC AGA AAC GGT AAC TTG GGT GCC C), the qPCR RD 5' forward (GGG AGA CCA CAA CGG TTT CCC), the qPCR-RD-L-5'-reverse (GCC GCT AGC CGC ACA GCT C), the qPCR-RD-tolA-3'-forward (GCC GAA TTC GGA TCT GGT GGC), the qPCR-RD-tolA-3'-reverse (CTG CTT CTT CCG CAG CTT TAG C), the qPCR-PD-pDX-forward (GAC GTT CCG GAC TAC GGT TCC), the qPCR-PD-pDX-reverse (CAC AGA CAG CCC TCA TAG TTA GC) were used to react qPCR of each step.

3. Ribosomal display

Incubate the mixture of components of the PUREfrex2.1 (GeneFrontier, PF213-0.25-EX), the oxidized glutathione (GSSG) and the disulfide bridge isomerase (DsbC) for 5 min at 37 °C using a PCR cyclor. Add 0.7 µl of the nanobody RNA library, corresponding to 1.6×10^{12} mRNA strands. Incubate the reactions for 30 minutes at 37 °C to form ribosomal complexes. Before making in vitro transcription of ribosome complex, prepare 10 ml of WTB-BSA (50 mM Tris/acetate pH 7.4, 150 mM NaCl, 50 mM MgAc₂, supplemented with

0.5% BSA), WTB-D (50 mM Tris/acetate pH 7.4, 150 mM NaCl, 50 mM MgAc₂, supplemented with 0.1% Tween20), WTB-D-BSA (WTB-BSA supplemented with 0.1% tween20). Place 12 µl of DynabeadsTMMyOneTMStreptavidinT1 bead (Invitrogen, 65601) in a 1.5 ml RNase-free/low binding microtube and place the tubes at magnetic rack on ice. Wash the beads twice with WTB-BSA using magnetic rack to immobilize the beads. Block the beads in WTB-BSA for > 20 minutes. The ribosomal complex is added to 100 µl of panning solution (WTB-D-BSA supplemented with 500 µg of heparin and 1µl of RNaseIn (Promega N2611), and then centrifuge the mix at 20,000×g for 5 minutes. The supernatant is mixed with biotinylated HER2 (Acro Biosystems, HE2-H82E2-200 µg) and incubated in the ice for 2 hours on ice to make complex ribosome and HER2. The magnetic bead is washed with WTB-B-BSA for three times, and the panning-HER2 mixture is added to the bead and subsequently incubate in the ice for 1 hour to bind biotin and streptavidin. The whole mixture is then washed with WTB-D for three times. The bonded nanobody RNAs are resuspended with RD elution buffer (50 mM Tris/acetate pH 7.4, 150 mM NaCl, 50 mM EDTA, and 100 µg/ml yeast RNA (Merck, R6750)) for 20 minutes at room temperature. The supernatant is purified by using RNeasy kit (Qiagen, 74004) with 15 µl of elution volume.

4. Reverse transcription

To make cDNA HER2 nanobody library, the eluted RNA from the Ribosomal display is reverse transcribed by using SuperiorScript III reverse transcriptase (Enzynomics, RT006M) with 30 µl of total volume, following the manual. The resulted cDNA is purified by using PCR purification mini kit (Favorgen, FAGCK 001-1) with 30 µl of elution volume. 2 µl of the resulted elution is used as a template of qPCR analysis, and 28 µl of the eluted solution is used for the amplification. The cDNA from DNA purification is amplified by PCR with Long_FX_For and Long_FX_Rev primers. The total reaction volume is 100 µl and then divided by two tubes when it starts the reaction.

5. qPCR

qPCR analysis is used for assessing the quality of the cDNA resulted from the ribosomal display and phage display selection to monitor the enrichment of the library during selection steps. qPCR is reacted by QuantStudio 3 Real-time PCR instrument (Applied Biosystems) with AccuPower® 2×Greenstar qPCR master mix (Bioneer, K-6251). The PCR program conditions are following; 95°C, 2 min (initial denaturation) / 95°C, 10 sec; 57°C, 30 sec; 63°C, 30 sec (Denaturation, anneal, elongate, measure) / melt curve step is followed default setting of the machine manual.

6. Making Electro component SS320 cell

To start transformation of Ribosomal Display output cDNA library, prepare an overnight culture of *E. coli* SS320 in TB medium supplemented with 10 µg/ml tetracycline, with shaking at 37°C. Inoculate 250 ml Erlenmeyer flask containing 200 ml TB medium (no antibiotic) with 2 ml of the overnight culture. Grow the cultures at 37°C while shaking at 160 rpm to an OD₆₀₀ of 0.4. Chill the cultures on ice for > 10 min. Centrifuge at 5,000×g for 10 min in sterilized buckets. Decant the supernatant and resuspend the pellets in 40 ml of ice-cold and sterile 1 mM HEPES pH 7.4. Centrifuge at 5,000×g for 10 min. Decant the supernatant and resuspend again using same volume of HEPES pH 7.4. Centrifuge at 5,000×g for 10 min. Decant the supernatant and resuspend the pellets in 20 ml of ice-cold and sterile 10% ultrapure glycerol. Centrifuge at 5,000×g for 10 min. Decant the supernatant and add 300 µl of ice-cold and sterile 10% ultrapure glycerol and resuspend the pellet. Transfer 350 µl aliquot in sterile 1.5 ml tubes and flash-freeze in liquid nitrogen. Store the frozen cells at −80°C.

7. Electroporation

To transfer FX cloning with RD output plasmid into SS320, thaw an aliquot of SS320 cells on ice, and place the ligation reaction and electroporation cuvettes with a 0.2-cm gap on ice as well. Mix the 50 µl ligation reaction with the competent cells by pipetting gently up and down. Pulse the cells with a BioRad Gen Pulser II electroporation system using 2.4 kV, 25 µF, and 300 Ω. After that, immediately transfer the electroporated cells to 25 ml of SOC medium. Incubate the culture at 37°C and 160 rpm for 30 min. Generate a

dilution of 25 μ l from the recovered culture by diluting six times 10-fold in LB media. Streak out 125 μ l of the dilutions on LB-agar plates containing 100 μ g/ml ampicillin to check the efficiency of the transformation. Transfer the rest of the culture into 225 ml of 2YT containing 100 μ g/ml ampicillin and 2% glucose and incubate overnight at 37°C and 160 rpm.

8. Production and purification of the phage

To prepare the phage for phage display, prepare 50 ml of 2YT containing 100 μ g/ml ampicillin and 2% glucose. Inoculate 1 ml of overnight culture of electroporated cells and grow the culture at 37°C and 160 rpm for 2hr until 0.6 of OD₆₀₀. Add 30 μ l of the M13K07 helper phage at 5×10^{12} pfu/ml in 10 ml of the culture and incubate at 37°C without shaking for 30 min. after that, centrifuge at 5,000 \times g for 10 min and resuspend the pellet in 50 ml 2YT containing 100 μ g/ml ampicillin and 25 μ g/ml kanamycin. Grow the culture at 37°C and 160 rpm for overnight to produce phage. Next day, centrifuge the overnight culture at 5,000 \times g for 30 min, 4°C. Transfer 40 ml of supernatant into a autoclaved 50 ml tube and add 10 ml of the PEG6000/NaCl solution and mix by inverting the tube. Incubate on ice for 2 hr to enrich the phage and centrifuge the mixture at 10,000 \times g for 1hr at 4°C. Resuspend the phage pellet in 300 μ l PBS and transfer into 1.5 ml tube. To remove the aggregates, centrifuge the resuspended phages at 20,000 \times g for 5 min two times. Measure the titer of the collected phage by using UV visible spectroscopy at 269 nm and 320 nm, then calculated using below formular.

$$Phages/ml = ((A_{269} - A_{320}) \times 6 \times 10^{16}) / 4900$$

9. Phage display

Before the phage display, prepare SS320 cells of seed cultures in 5 ml of 2YT with 10 μ g/ml tetracycline for overnight and coat 48 wells of 96 well plate with 100 μ l of 67 nM neutravidin in 4°C. and then, inoculate 1 ml of the overnight culture in 50 ml 2YT with 10 μ g/ml tetracycline. To start first phage display, prepare 50 ml TBS, TBS-BSA (TBS supplemented with 0.5% BSA), TBS-BSA-D (TBS supplemented with 0.5% BSA, and

0.1% tween 20), 150 ml of TBS-D (TBS supplemented with 0.1% tween 20). Wash the coated plate once with 250 μ l of TBS per well and block the wells with 250 μ l of TBS-BSA for 30 min and prepare 5 ml of TBS-BSA-D containing 5×10^{12} phage from phage production and purification steps. Transfer 100 μ l of the phage mixture in 1.5 ml tube to make negative control. Add the biotinylated HER2 to the rest of phage mixture at 50 nM and mix well and add biotinylated MBP (negative control) to 100 μ l of the phage mixture. Incubate the mixtures for 2 hr at room temperature to make complex of HER2 and phages. Wash the plates once with 250 μ l of TBS-BSA-D per well and transfer the HER2-phage mixture to 47 wells and the negative control to rest well. Incubate 1 hr to make complex neutravidin-HER2-phage. Wash the wells with 250 μ l of TBS-D for three times and dried on the paper tissue every washing step for 2 min. Add 100 μ l of PD elution buffer (TBS supplemented with 0.25 mg/ml trypsin) to each well and incubate for 10 min at room temperature. To inhibit activation of trypsin, add the AEBSF solution and 2 μ l of the elution is used for qPCR analysis to check output phage amount compared input phages. Add 45 ml of the inoculated culture to the rest of elution and incubate at 37°C for 30 min without shaking to infect the cells. After that, mix the infected culture with 200 ml of 2YT containing 100 μ g/ml ampicillin and 2% glucose and incubate at 37°C and 160 rpm for overnight. To start second phage display, prepare 200 μ l phage solution containing 5×10^{12} phages from the first phage display output amplified by phage production and purification steps and 10 ml of TBS-BSA, TBS-BSA-D, TBS-D. 12 μ l of Dynabeads™MyOne™StreptavidinC1 bead (Invitrogen, 65001) is placed in 1.5 ml tube, washed twice with 500 μ l of TBS-BSA using magnetic rack and blocked with 500 μ l of TBS-BSA for >20 min. To make panning solution, mix 100 μ l of the phage solution and 50 nM of biotinylated HER2 and mix rest of solution and biotinylated MBP (negative control). Incubate the mixtures for 2 hr then wash the beads three times with TBS-BS-D. Beads were resuspend with 100 μ l of panning solutions and incubate for 1 hr then wash the beads once with TBS-BSA-D. To select the HER2 specific phage, add 100 μ l of the competition buffer containing 5 μ M non-biotinylated HER2 in each tube and incubate for 3 min. After washing twice with TBS-D, add 100 μ l of PD elution buffer and incubate for 10 min at room temperature. Then, treat AEBSF to the elution buffer to inhibit activation of trypsin and 2 μ l of mixture is used for qPCR analysis. Rest of the solution is mixed

with 1 ml of SS320 to infect the output phages and cultured in 2YT media with 100 µg/ml ampicillin and 2 % glucose at 37°C and 160 rpm for overnight.

10. Cell binding assay using output phages from each Phage Display

To check that the output phages from each step are enriched into HER2, start binding assay using HER2 overexpressed SNU-1 HER2 Knockdown SNU-1. Each 10^5 cell is mixed with 10^{10} phages of each first output and second output on ice and wash twice with PBS. Add 100 µl of PBS containing 1:2,000 diluted anti-M13-mouse antibody (SinoBiological, 11973-MM05T) in washed cells, resuspend the cells and incubate on ice for 30 min. Wash twice with PBS and add 100 µl of PBS containing 1:2,000 diluted anti mouse Alexa 647 goat antibody. Incubate it on ice for 30 min. after washing twice, a total of 10^4 cells are counted by flow cytometry (FACS LSR II, BD Biosciences) and analyzed with Flow-Jo software.

11. ELISA

After transforming clones from FX cloning using pSBinit vector (Addgene, 110100) to BL21 by heat shock and streak it on LB-agar plate with 25 µg/ml chloramphenicol, 200 colonies were cultured in prepared 2 ml TB media at 37°C and 220 rpm until the $OD_{600} = 0.4\sim 0.8$ and cultivated at 22°C and 150 rpm. Negative control MBP colony is cultured in the same way. Then, each culture is treated with 0.02% of L-(+)-arabinose and incubate at 22°C and 150 rpm for overnight to produce nanobody. After using periplasmic extraction buffer (20% sucrose, 50 mM Tris pH8.0, 0.5 mM EDTA, and 0.5 µg/ml lysozyme in DW), extract nanobodies from pellets and load 20 µl of solutions treated with 6x sample buffer in 12% SDS-PAGE-GEL to determine which colonies expressed nanobody. After checking gel results, choose 96 of the colonies that expressed nanobody. To find nanobody that binds specifically to HER2, prepare the plate coated with 100 µl of 5 µg/ml protein A solution and incubated in 4°C for overnight with adhesive sealing before one day. Then, wash the plate once with 200 µl of TBS per well and block it with TBS-BSA for 30 min. Add 100 µl of a 1:2,000 diluted anti-c-Myc mouse antibody (Biolegend, 626802) in TBS-BSA-D per well and incubate for 20 min. after washing three times with 200 µl of TBS-D, 80 µl of TBS-BSA-D is added per well and 20 µl of the periplasmic

extraction is added side by side and incubate for 20 min to compare the binding rate of the nanobody between HER2 and MBP. After washing three times it with 200 μ l of TBS-D per well, add 100 μ l of the biotinylated HER2 and negative control at 50 nM in TBS-BSA-D to the respective wells and incubate for 20 min. After washing three times it with 200 μ l of TBS-D per well, treat 100 μ l of 1:5,000 diluted streptavidin-peroxidase (Invitrogen, 434323) in TBS-BSA-D per well and incubate for 20 min. Wash again three times with 200 μ l of TBS-D per well and add 100 μ l of TMB substrate (Biolegend, 421101) to each well. The reaction will take approximately 15 minutes, until individual wells turn blue. The absorbance is measured at 650 nm in the plate reader every 5 min.

12. Production and purification of the nanobodies

Nanobody clone that was considered positive candidate from ELISA result is transformed into the *E. coli* BL21 and cultured in 37°C, 160 rpm for overnight. 2 ml of 5 ml of the overnight culture is inoculated into the 200 ml of TB medium supplemented with 25 μ g/ml of chloramphenicol, and cultured in 37°C, 200 rpm until OD₆₀₀ = 0.6. And then, start cultivation at 22°C, 150 rpm for 1 hr and treat 0.02% of arabinose, and culture in 37°C, 150 rpm for overnight. Centrifuge the culture at 5,000 \times g, 4°C for 15 minutes, resuspend the pellet with 20 ml of the periplasmic extraction buffer in the ice for 30 minutes. After the incubation, add 180 ml of TBS supplemented with 1 mM MgCl₂ and centrifuge it at 5,000 \times g, 4°C for 15 minutes. After that, transfer supernatants into 50 ml tube by dividing it. To purify the nanobody, 1ml of TALON®Superflow™ (Cytiva, 28957502) slurry is pre-equilibrated with TBS pH 8.0 and incubated with periplasmic extract solution in 4°C for 1 hour with gentle rotation. After the binding, wash the beads with the washing buffer (50 mM Tris pH 8.0, 300 mM NaCl, and 5 mM imidazole) for three times, and then elute the nanobody by using the elution buffer (50 mM Tris pH 8.0, 300 mM NaCl, and 200 mM imidazole). The eluted nanobody need to the buffer change by using Slide-A-Lyzer® Dialysis Cassette (Thermo, 66330) for overnight.

13. Cloning HER2-EGFP

To check endocytosis using mono-nanobody, multi-paratopic nanobody, clone of HER2 ECD-TM-EGFP is made from pLX 304-ERBB2 plasmid using PCR and ligation with

digested EGFP-N1 plasmid by XbaI, AgeI enzyme. To check expression of clone, transfect it to the SNU-1 cell for 48 hr and check fluorescence by using fluorescent inverted microscope (OLYMPUS, IX71/DP71).

14. HER2 Domain expression

To distinguish binding site of nanobodies, clone of MBP-HER2 domains (II+III+IV, III+IV, IV) is made from MBP plasmid using PCR. To expression that, BL21 was transformed and induced by IPTG 0.3 mM at 22°C, 150 rpm for overnight. To purify this, Sonication was started into pellet including MBP binding buffer. And then, washing step was started in using column and purified by Elution buffer containing 10 mM maltose.

15. *In-silico* nanobody prediction

To predict the nanobody structure, AlphaFold2, RosettaFold2, OmegaFold2, Nano-Net was performed. After comparing these result, ERRAT score was compared. The highest score model was analyzed by Ramachandran plot.

16. *In-silico* HER2-nanobody Docking prediction

To make optimal multi-paratopic nanobody, we use computational method and cell-based method. HDock, HADDOCK docking program, computational method, predicts model of protein-protein interaction. According to computational method, we construct structure of each domain-nanobody interaction and find optimal binding site of nanobodies. Then, we design multivalent nanobody against a various combination of structure which is composed of each HER2 domain. The interactions between each combination and HER2 full ectodomain are evaluated successively by analyzing distance between domains by superimposing each docking models by using Pymol, interaction bond such as hydrogen bond each other using ChimeraX-1.5 program that can analysis structure.

17. HER2 crystal structure analysis

To predict binding epitope, HER2 (PDB: 6J71) solvent accessible surface area (SASA) was performed. And candidate binding epitopes that has over SASA 60% were specified to compare docking score by HADDOCK. And then, HER2 height was analyzed to

compare between HER2 active form and endocytosis form. Additionally, HER2-Domain II dimerization arm change was performed by superimposing 6 HER2 crystal structures (PDB: 7MN6, 1N8Z, 8HGO, 7MN5, 1S78, 8FFJ). All of the HER2 structure analysis was performed by using Pymol program.

18. Making multi-paratopic nanobody

Based on the results of *in vitro* and *in-silico*, each nanobody for each domain binding site was confirmed. A multi-paratopic nanobody design was performed by measuring the distance of each nanobody, and G4S(n) amino acid linker was nominated. To express multi-paratopic nanobody, clones were made in pSB-vector. Then, express these clones in BL21 and purify them through His-resin.

19. Binding assay

To check HER2 expression of 3 types of gastric cancer cells, 2×10^5 cells per tube are suspended in 100 μ l of PBS, and antibodies are treated with 70 nM and incubate at 4°C for 1 hr. After washing three times with PBS, 100 μ l PBS was treated with a goat anti-human Ig Fc-specific Alexa 680-conjugated secondary antibody (109-605-003, Jackson) at 1:500 dilution and incubate at 4°C for 1 hr. After washing three times with PBS, a total of 10,000 cells are counted by flow cytometry (FACS LSR II, BD Biosciences) and analyzed with Flow-Jo software.

20. Amin conjugation pH sensing dye to antibody

To make pH-sensing fluorescent antibody to check endocytosis rate, exchange the antibody buffer to the amine conjugation buffer using a desalting column (Zeba TM Spin Desalting Columns, 7K MWCO, 0.5 ml; Thermo Fisher scientific, 89882) Add 1.2 μ l of pHAb Amine Reactive Dye (Promega, G9845) for 100 μ g of antibody to make a 20-molar excess of dye. Incubate for 1 hr with mixing at room temperature. And remove the unreacted dye using desalting column. After that, calculate the antibody concentration and dye-to-antibody ratio using below formular.

21. Checking endocytosis

To check endocytosis rate by using pHAb, incubate 1×10^5 cells with 70 nM antibody conjugated with pH-sensing dye at 37°C for 24 hr and wash two times with PBS by centrifuging at 2000 rpm for 2 min. Resuspend the cells in 200 μ l PBS. A total of 10,000 cells are counted by flow cytometry (FACS LSR II, BD Biosciences) and analyzed with FlowJo software.

22. Confocal image

To find that HER2 mediated endocytosis is followed by lysosome pathway, incubate 2×10^5 cells with 70 nM antibody conjugated with pH-sensing dye at 37°C for 24 hr and wash two times with PBS by centrifuging at 2000 rpm for 2 min. After washing, treat LysoTracker Deep Red 100 nM for 2 hr and incubate at 37 °C and 5% CO₂ incubator. After wash two times with PBS, resuspend cells, fix at room temperature for 10 min with 4% Formaldehyde. After washing 3 times with PBS, treat PBS containing DAPI diluted 1:5000 for 5 min. After washing 3 times with PBS, mix with mounting media, place on slide glass. After cover with 12 mm round coverslip, observe by confocal microscopy.

23. Cell viability

Incubate 1×10^4 cells per 100 μ l RPMI with T-DM1 each dose in opaque walled 96 well plates at 37°C for 72 hr and equilibrate the plate and its contents to room temperature for approximately 30 min. Add 30 μ l of Cell Titer-Glo® 2.0 Reagent (Promega, G9241) in each well. Mix the contents for 2 min on an orbital shaker to induce cell lysis and incubate at room temperature for 10 min to stabilize the luminescent signal. Record luminescence by using luminescence spectrophotometer (LS50B, Perkin Elmer).

24. Lentivirus production

Before one day, Seed 0.8×10^6 HEK293T cells per 2 ml DMEM in 6-well plates at 37°C for 24 hr and exchange new pre warmed media. Incubate by co-transfection of clone pDNA and lentivirus component DNA clone pMD2G and psPAX2 into HEK293T cells using PEI (polyethylenimine) transfection reagent. After overnight, change the cell culture solution. After 48 hr, the cell culture solution was separated and centrifuged at 4°C for

2000 rpm for 5 min, and only the supernatant was transferred to a clean tube to remove the mixed cells. Store it at 4°C for 1 week.

25. Generation of GFP-dCas9-SNU-1 cell

To make genome knockdown system, incubate 5×10^4 cells per 1 ml RPMI with lentivirus to infect pLV hUbc-dCas9-T2A-GFP plasmid (Addgene, #53191) in 12-well plates at 37°C for 24 hr and exchange 1 ml of new media. Rescue for 2 days, the GFP positive cells is sorted by flow cytometry (FACS Aria III, BD Bioscience).

26. Generation of HER2 overexpression cell

To make positive HER2 overexpression cell, incubate 5×10^4 cells per 1 ml RPMI with lentivirus to infect pLX304-ERBB2 plasmid (Addgene, #175846) in 12-well plates at 37°C for 24 hr and exchange 1 ml of new media. Rescue for 1 days and treat 5 µg/ml blasticidin (Biomax, SMB001-100MGS) for 2 days.

27. Cloning of CRISPRi ERBB2 sgRNA

To make Oligo hybridization of two single strands with complementary bonds containing ERBB2 sgRNA sequence 5'-GTTGGGACCGGAGAAACCAG-3', phosphorylate and anneal each pair of oligos by using T4 PNK and put the phosphorylation/annealing reaction in a thermocycler program; 37°C 30 min / 95°C 5 min and ramp down to 25°C at 5°C/min. Then, set up ligation reaction solution containing oligo-hybridization products, T4 ligase, pCRISPRi-v2 vector that was cut by BstXI (Thermo Fisher scientific, ER1022), Bpu1102I (Thermo Fisher scientific, ER0092) and incubate at room temperature for overnight

28. HER2 Knockdown using CRSPRi system

Incubate 5×10^4 cells per 1 ml RPMI with lentivirus to infect pCRISPRi-v2 (Addgene, #84832) containing ERBB2 sgRNA sequence in 12-well plates at 37°C for 24 hr and exchange 1 ml of new media. Rescue for 1 days and treat 0.75 µg/ml puromycin (Invitrogen, ant-pr-1 100MG) for 2 days. A total of 10,000 cells are counted by flow cytometry (FACS LSR II, BD Biosciences) and analyzed with Flow-Jo software.

29. Bio-layer Interferometry (BLI)

The measurement of nanobody binding affinity was conducted using a Gator Prime Instrument (Gator Bio). To immobilize the biotinylated antigen, streptavidin biosensors (SA) were employed. The entire process, including baseline establishment, loading of the antigen, association with nanobody, and dissociation, was performed in wells of a black polypropylene 96-well microplate. To prevent non-specific binding to the SA sensor, a reaction buffer containing 0.02% Tween-20 and 0.1% BSA was employed. The binding affinity measurement followed a specific experimental protocol: a 60-second baseline, 120 seconds of antigen binding on the SA sensor, another 60-second baseline, followed by 150 seconds of association with the nanobody and 150 seconds of dissociation at 1000 rpm. The obtained binding data were fitted to a 1:1 homogeneous ligand model, and steady-state analysis was carried out to derive the binding kinetics parameters, including the dissociation constant (KD).

30. Epitope binning using BLI

Similarly, the streptavidin biosensor (SA sensor) and biotinylated antigen were utilized for the binning step. The binning protocol involved a 60-second baseline, followed by 120 seconds of antigen binding. Subsequently, another 60-second baseline was established, followed by 580 seconds of the first nanobody binding and an additional 400 seconds of the second nanobody binding. During the second nanobody binding step, the buffer for the second nanobody contained the same concentration as the first nanobody to prevent the binding of the second nanobody to the dissociated first nanobody epitope space. This strategic approach ensures the specificity of binding and accurate assessment of the nanobodies' interactions with the antigen.

31. Cloning of multi-paratopic nanobody

To generate nanobody secretion vector that was modified to pSport6 vector, first nanobody was conducted on PCR with forward primer containing SpeI enzyme site and reverse

primer containing Esp3I-(G₄S)₁ or Esp3I-(G₄S)₃. Second nanobody was reacted with forward primer containing Esp3I and reverse primer containing Esp3I-(G₄S)₁ or Esp3I-(G₄S)₃ that was base sequence modified to cognize only third nanobody. Third nanobody was reacted with Esp3I forward primer -modified sequence to cognize only this and BamHI-reverse primer. These PCR product and enzyme cut vectors were ligated with T4 DNA ligase (Enzynomics, M001S).

32. Expression of multi-paratopic nanobody

To transiently express the multi-paratopic nanobody, HEK293T cells were utilized. A total of 3.5×10^6 cells were seeded in a 100 μ l cell culture plate with DMEM media one day prior and then incubated at 37°C in a 5% CO₂ incubator. Subsequently, 10 μ g of plasmid containing the multi-paratopic nanobody gene was combined with PEI (DNA: PEI = 1:3) and incubated for 15 minutes at room temperature. This solution was then mixed with the media containing living cells and incubated for 6 hours, followed by the addition of 5 ml of new culture media. The following day, the cells were washed with PBS, and the media was replaced with 10 ml of freestyle media (Gibco™, 12338018), and the cells were further incubated for 4 days.

33. Antibody purification

To purify the FC-fusion protein, start by preparing a solution containing 0.1 M citric acid, 1 M Tris, and PBS at either ice temperature or 4°C. Depending on the antibody concentration, ready the protein A beads (Pierce™ Protein A Agarose, 20334). Add the required amount or 100 μ l of bead slurry to 1 ml of PBS in an e-tube. Wash the bead storage buffer by inverting or using a rotator for 5 minutes at 4°C, followed by centrifugation at 2000 RPM for 3 minutes. Discard the supernatant, resuspend the beads with 1 ml of PBS, and repeat the process. Discard the supernatant once more, resuspend the beads with 1ml of 293 Freestyle media, and allow equilibration for 5 minutes using a rotator (or 293

Freestyle media). Add the beads containing the antibody to the media. Using a rotator, incubate the antibody with beads for 2~4 hours at 4°C or overnight. Activate the column by adding 5 ml of cold PBS. Place the bead-containing antibody media into the column to collect antibodies. Wash the bead pellet in the column by adding 7 ml of cold PBS (repeat twice). Add 25 µl of 1M Tris to the filtered solution in an Epi tube for neutralizing the eluted antibodies. To elute antibodies, add 75 µl of 0.1 M citric acid solution to the column, incubate for 1 minute, and collect the eluted antibodies in e-tubes for further processing.

34. Statistical analysis

Statistical analyses were conducted using Prism v9 (GraphPad Software). The data are expressed as means ± standard deviation, as specified in the figure legends. Statistical significance was evaluated using Student's multiple unpaired t-test. Significance levels are denoted as follows: * $p < 0.05$.

III. RESULTS

1. Low effect of Trastuzumab in low HER2 gastric cancer

ERBB2 transcription rate data indicated lower levels in gastric cancer cells compared to breast cancer cells (Fig. 1A). To assess endocytosis rates in cells with varying HER2 expression, we synthesized trastuzumab conjugated with a pH-sensing dye. Its functionality was validated through pH exchange (Fig. 1B). Using this, we discovered that endocytosis is correlated with HER2 expression levels, as observed with flow cytometry (Fig. 1C) and confocal microscopy (Fig. 1D). We employed Lysotracker to track whether trastuzumab is trafficked to lysosomes. The images demonstrated co-localization of trastuzumab and lysosomes, with a more pronounced effect in cells expressing higher levels of HER2. To assess the impact on antibody-drug conjugates (ADCs), we utilized T-DM1 conjugated with emtansine. Consequently, only cell lines expressing substantial HER2 exhibited greater cellular toxicity effects than those with lower HER2 expression (Fig. 1E). Numerous studies have explored strategies to enhance endocytosis by targeting different domains of HER2^{13, 15}. Given this, we have decided to develop nanobodies targeting multiple domains to augment endocytosis.

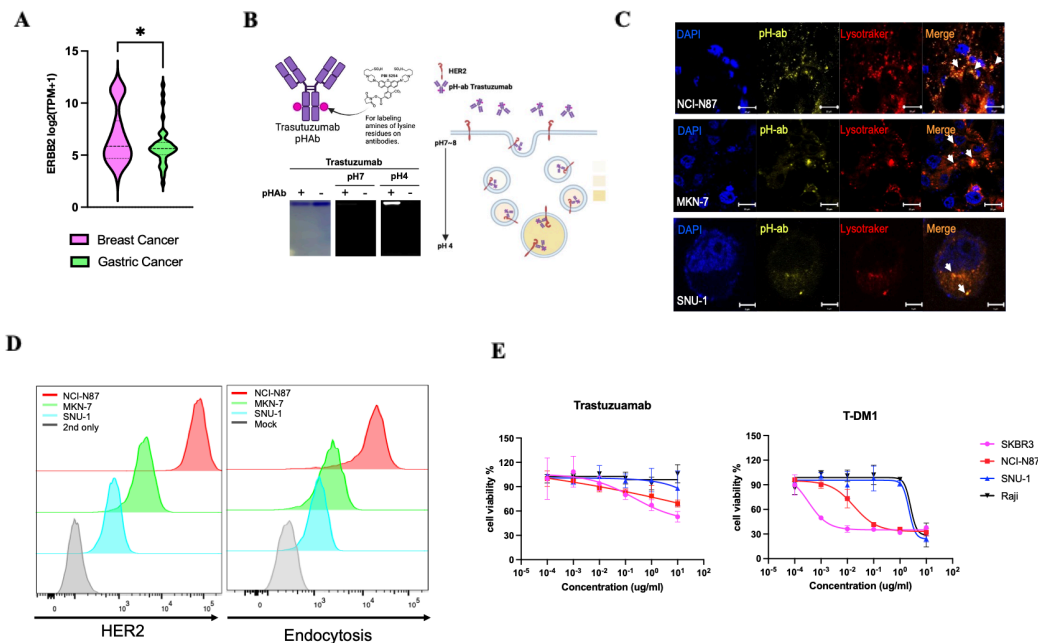


Figure 1. HER2 expression & endocytosis in gastric cancer. (A)ERBB2 expression log₂ (TPM+1) transcription per kilobase million data of Breast cancer cells (n=61) & Gastric cancer cells (n=41) in The Cancer Dependency Map (DepMap) on 2022Q. (unpaired t-test, $p=0.0412$) TPM is meaning Transcripts Per Million, normalizes all the reads within a run so that the sum of all the reads would be exactly 1,000,000. **(B)** Trastuzumab conjugated with pH-sensing dye and validation of function. **(C)** Confocal image of 3 GC cell lines. Trastuzumab pH-ab concentration 1 μ g/ml and incubation for 22 hr, LysoTracker Deep Red (Thermo Fisher, #L12492) 100 nM for 2 hr in each well. **(D)** Binding assay treated with trastuzumab (1 μ g/ml) to check HER2 expression (left) and endocytosis treated with pH-ab (1 μ g/ml) to Check HER2 internalization (right) in 3 GC cells by using flow cytometry. **(E)** Cell viability by treatment of trastuzumab, T-DM1 (ADC of trastuzumab) for 48 hr.

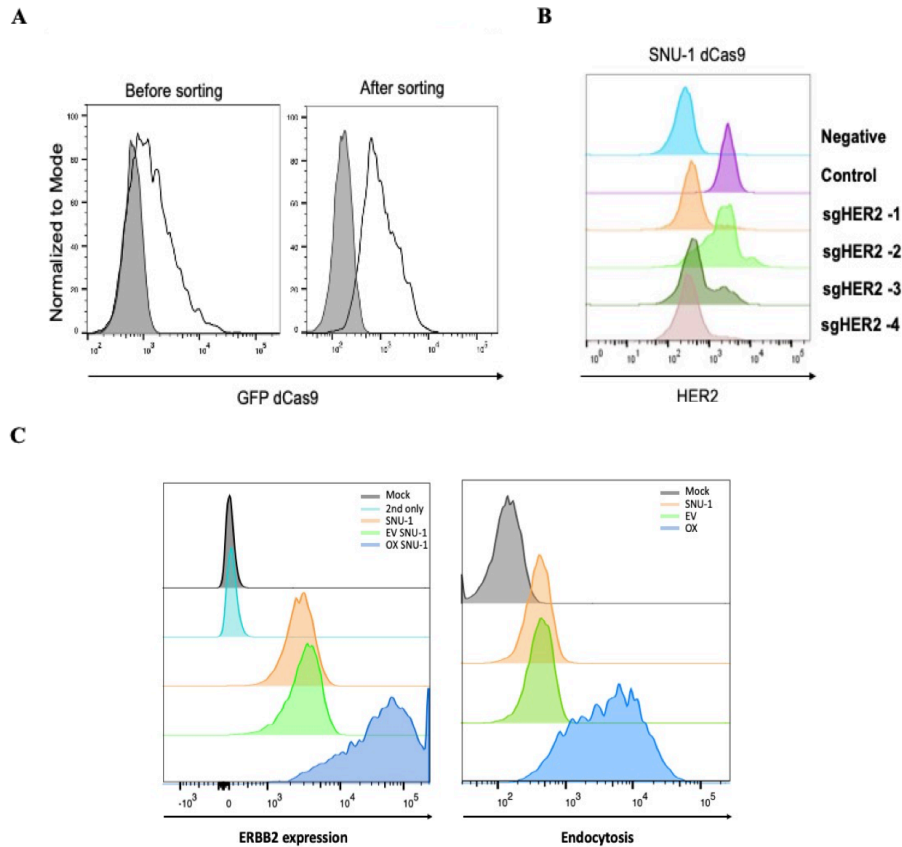
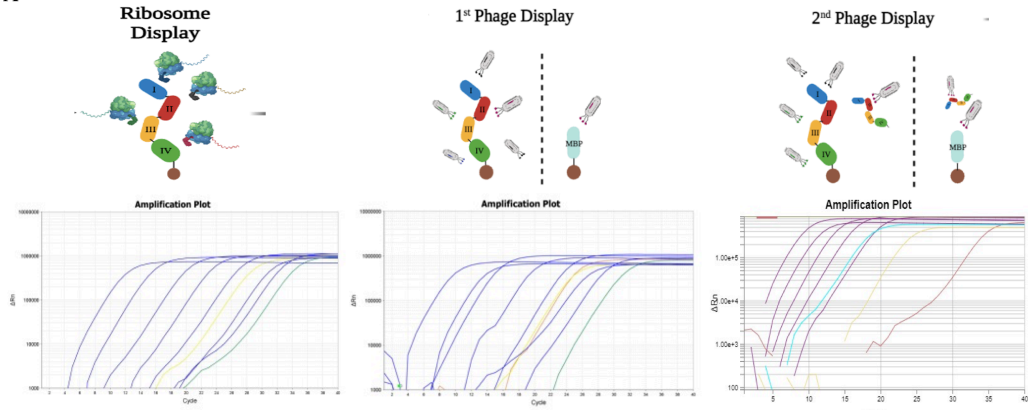


Figure 2. Generation of HER2 knockdown & overexpression cell line. (A) Enrichment of dCas9-GFP stable cell. (B) Cell binding assay to validate HER2 knockdown. (C) Cell binding assay and endocytosis rate to validate HER2 overexpression with trastuzumab 1 $\mu\text{g/ml}$. EV means empty vector, OX means overexpression.

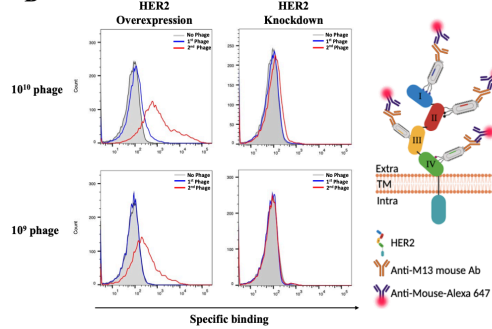
2. Screening of anti-HER2 nanobody

A synthetic nanobody targeting the extracellular domain of HER2 was discovered through a series of screening processes, including ribosome display, two rounds of phage display, and ELISA. The diversity of the nanobody library pool was estimated during screening using quantitative PCR (Fig. 3A). We initiated ribosomal display with a library pool size of 1.6×10^{12} , resulting in a display mRNA diversity of 3.2×10^7 . After the first and second rounds of phage display, we observed a 238-fold increase in positive phage compared to negative phage. To confirm the enrichment of phage clones, we conducted a phage binding assay using HER2 overexpressing and knockdown cells (Fig. 3B). The knockdown (KD) cells were generated using CRISPRi-dCas9 (Fig. 2A, B), while the overexpressing (OX) cells were created through a lentiviral system (Fig. 2C). In OX cell, second phage display output got highly binding affinity than first phage display output. Unlikely this, both outputs were not bound to KD cell. So, we could check that this process was going well. To identify clones with proper periplasmic expression, we assessed the nanobody expression of 115 clones using SDS-PAGE gel staining (Fig. 3C). Out of these clones, 97 exhibited expression and proceeded to the ELISA screening step. Following the ELISA screening, 17 clones were selected as promising candidates, displaying at least a 1.5-fold higher binding response to HER2 compared to the negative control target (MBP) in ELISA (Fig. 3D).

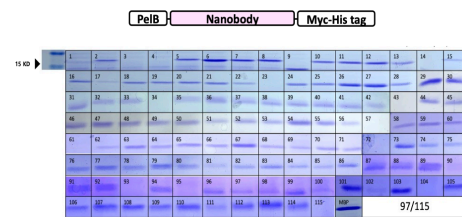
A



B



C



D

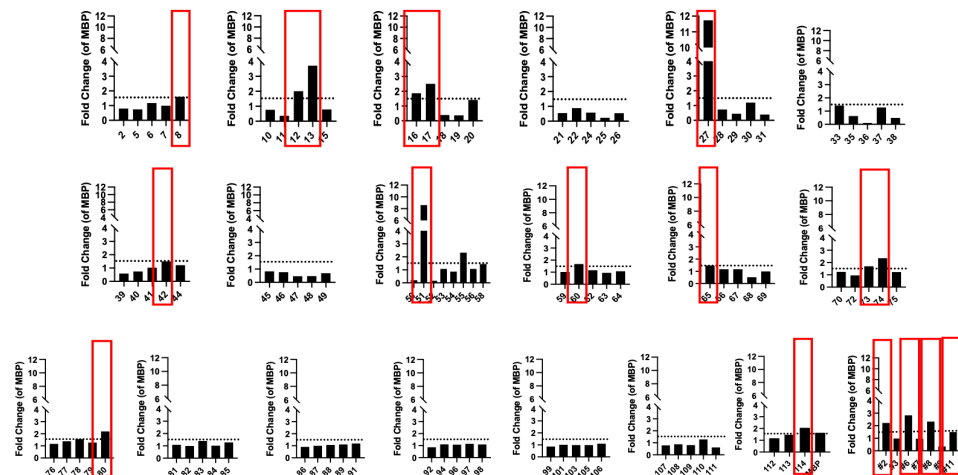
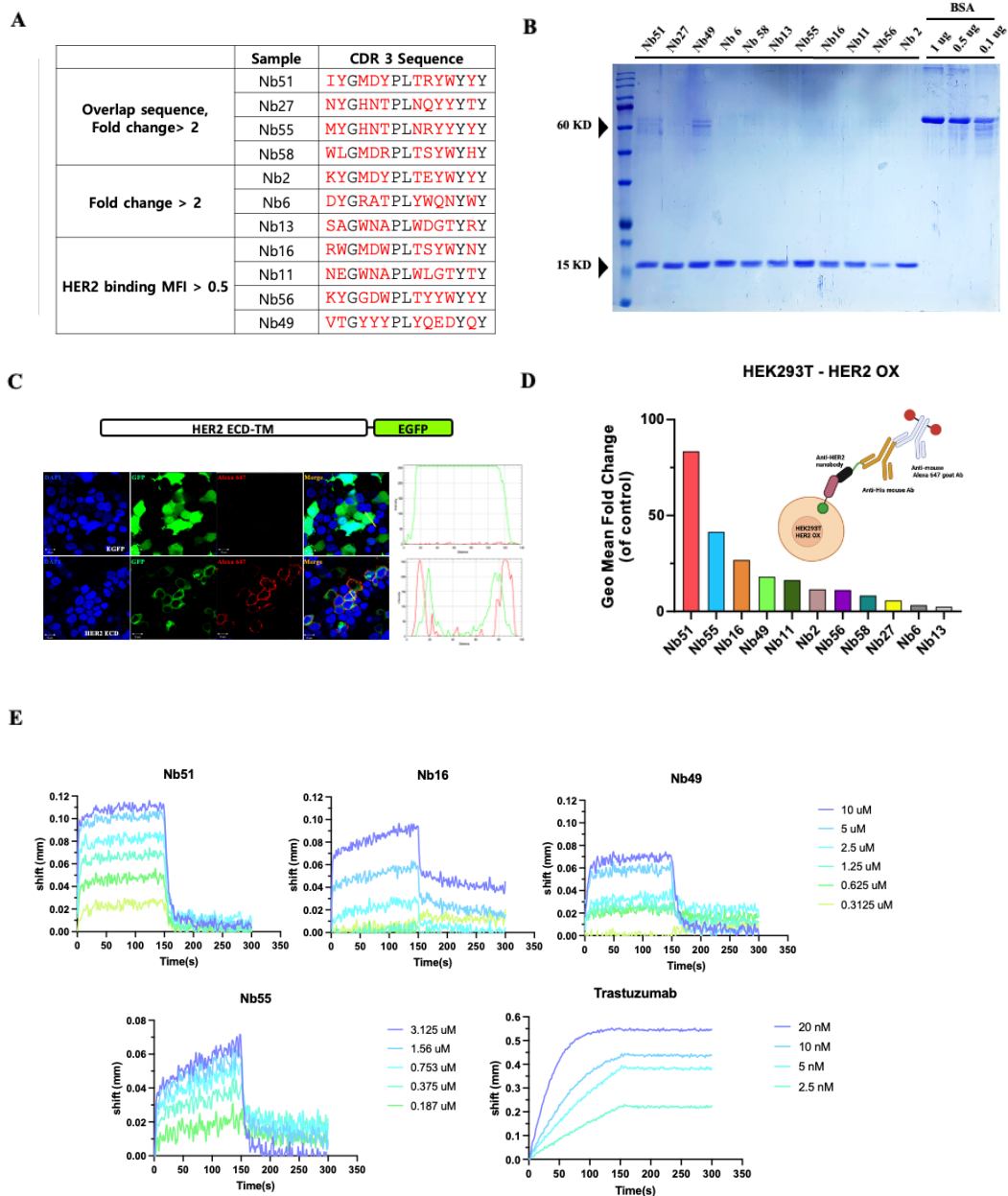


Figure 3. Screening of synthetic nanobody against the HER2. (A) Screening process for discovering anti-HER2 nanobody. Diversity of the library pool was approximated after each step by quantitative PCR. (B) Phage binding against HER2 OX and HER KD cell line. Anti-M13-mouse antibody was used to detect nanobody and anti-mouse-Alexa 647 was used to detect mouse antibody. (C) Result of periplasmic protein expression of 115 nanobody clones through SDS-PAGE gel staining. (D) ELISA result for determining the nanobodies which have specific binding affinity to the HER2. Fold-change refers a difference of nanobody's binding between HER2 and MBP.

3. Purification and binding of nanobody

To reduce the number of candidates, we categorized the nanobodies into three conditions (Fig. 4A). We found that there were 4 nanobodies with overlapping sequences and a Fold Change (FC) > 2, 3 nanobodies with only FC > 2, and 4 nanobodies with a target binding Mean Fluorescence Intensity (MFI) > 0.5 and FC > 1.5. Consequently, we selected a total of 11 nanobodies meeting these criteria and proceeded to purify them using a His-resin purification method (Fig. 4B). To assess the cell binding affinity of each nanobody, we generated HEK293T cells transiently expressing the HER2 ectodomain with EGFP instead of the intracellular domain (Fig. 4C). Trastuzumab was used to confirm the successful expression of recombinant HER2 protein. We employed anti-human FC-Alexa 647 to visualize the binding using a confocal microscope. Compared to the negative control, HER2-ECD-EGFP translocated to the cell membrane. The fluorescence histogram indicated that trastuzumab bound to the outer membrane expressing HER2-ECD, while EGFP illuminated the inner membrane in the cytosolic region. Using this methodology, we conducted a cell binding assay employing a flow cytometer (Fig. 4D). Notably, Nb51 exhibited the highest binding affinity among all tested nanobodies in flow cytometry. Accordingly, we selected four nanobodies in descending order of their binding affinity results. To validate the binding affinity of the selected nanobodies, bio-layer interferometry (BLI) was employed (Fig 4E). The K_D values were determined as follows: Nb51 (5.97 nM), Nb16 (1.93 nM), Nb49 (1.33 μ M), Nb55 (4.46 nM), and the positive control trastuzumab (32.4 pM) (Fig 4F). Interestingly, although Nb51 exhibited the highest binding affinity in the cell binding assay, it had a relatively low K_D value compared to Nb16 in BLI. This result led us to consider that both k_{on} and k_{off} values play crucial roles in determining binding affinity.



F

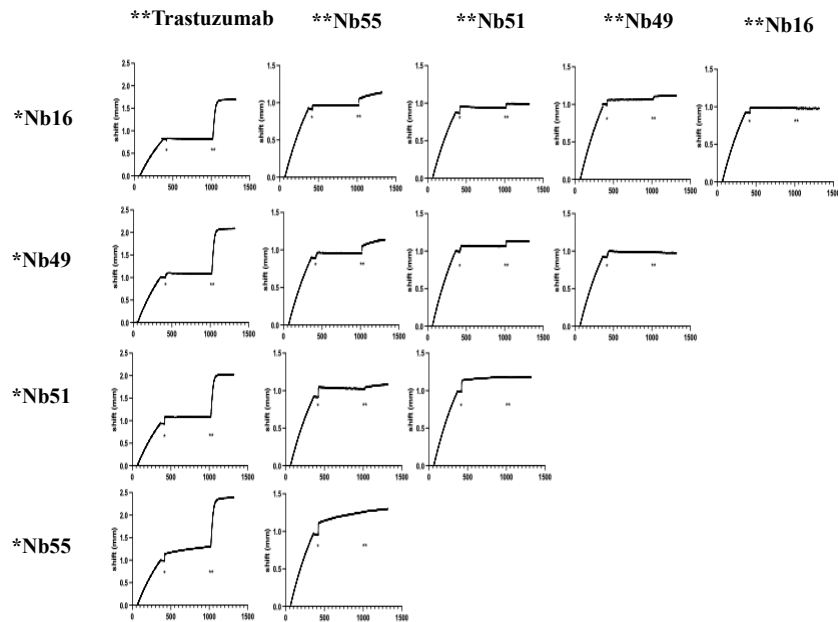
	$k_{\text{off}}(1/\text{s})$	$k_{\text{on}}(1/\text{Ms})$	$K_D(\text{M})$
Trastuzumab	3.98E-05	1.23E+06	3.24E-11
Nb51	0.106	1.78E+05	5.97E-07
Nb16	0.00962	4.97E+04	1.93E-07
Nb49	0.0407	3.05E+04	1.33E-06
Nb55	0.022	4.93E+04	4.46E-07

Figure 4. Purification and assesment binding affinity. (A) Amino acid sequences of nanobody's CDR3 resulted from the screening against the HER2. Randomized region is indicated as red. (B) The 11 different nanobodies targeting HER2 were subjected to SDS PAGE under reducing condition. BSA molecules were used as standard. (C) The HER2-ECD-EGFP was transiently expressed in HEK293T cell. The trastuzumab was used to validate this cell using confocal microscope and fluorescence line plot. GFP cell was used to negative. (D) The nanobodies cell binding affinity were confirmed in HER2-ECD-EGFP transiently expressed cell. The fold change was calculated compare to negative control. (E) Bio-Layer-Interferomerty, BLI results of nanobodies. (F) $K_D(\text{M})$ result chart of each nanobody and trastuzumab.

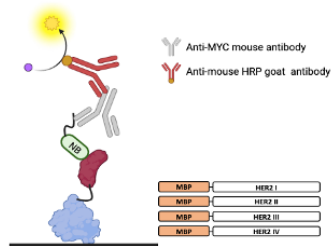
4. The distinction of nanobodies binding each domain

To check whether each nanobody shared binding with each other, epitope binning was started. Interestingly, they each did not share binding domain and also trastuzumab binding site (Fig 5A). As a point of note, The Nb55 showed a tendency to continue binding over time and was excluded because it was unclear what negative effects this might have. To identify the binding domains of the nanobodies, we produced MBP-Domain I, II, III, and IV fusion proteins using BL21 and subsequently purified them using exellose resin. These fusion proteins were then employed in an ELISA assay (Fig. 5B, C). Notably, Nb51 was found to specifically bind to Domain I, while Nb16 and Nb49 demonstrated binding to Domain II and Domain III, respectively. As expected, our positive control, Trastuzumab, exhibited binding affinity to Domain IV (Fig. 5D). In our pursuit of designing multivalent nanobodies, we initiated a predictive modeling process. *In-silico* methods, especially in the domain of protein-protein docking simulations for predicting binding sites, have gained prominence. AlphaFold 2 has received acclaim for its accuracy in monoprotein structure predictions, distinguishing itself among various structure prediction servers. Additionally, HADDOCK employs artificial intelligence to predict and generate protein-protein docking models²³, while HDock relies on knowledge-based data for the same purpose²⁴. We utilized the nanobody prediction server, AlphaFold 2, which demonstrated a higher ERRAT score than other servers (Fig. 5E, F) and over 90% accuracy in most favored regions (Fig. G). We also leveraged docking model prediction servers, namely HDock and HADDOCK and established specific criteria for docking energy scores to select the most promising candidates: the values lower than -300 for HDock and under -75 for HADDOCK (Fig. 5H). By comparing results from various docking servers, we successfully identified the binding domains of each nanobody. These predictions gained strong credibility, further supported by the crystal structure of the 2Rs15d case, which had previously been determined to bind to HER2 Domain I (Fig. 5I, Table 1). Importantly, our in-vitro and *in-silico* results were nearly corresponded.

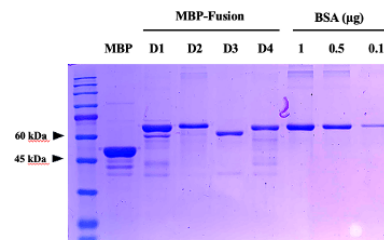
A



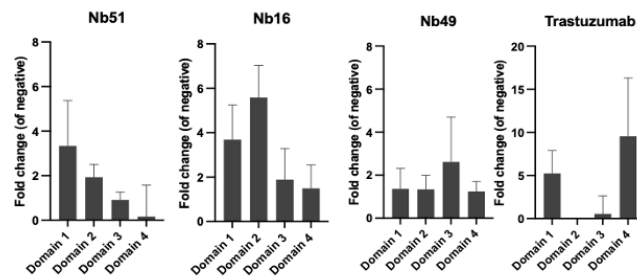
B



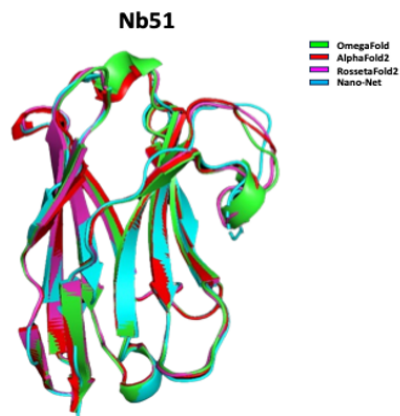
C



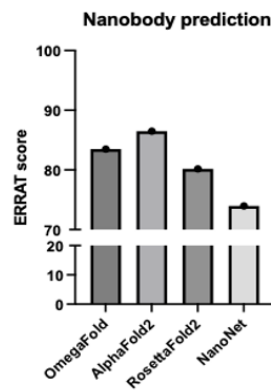
D



E



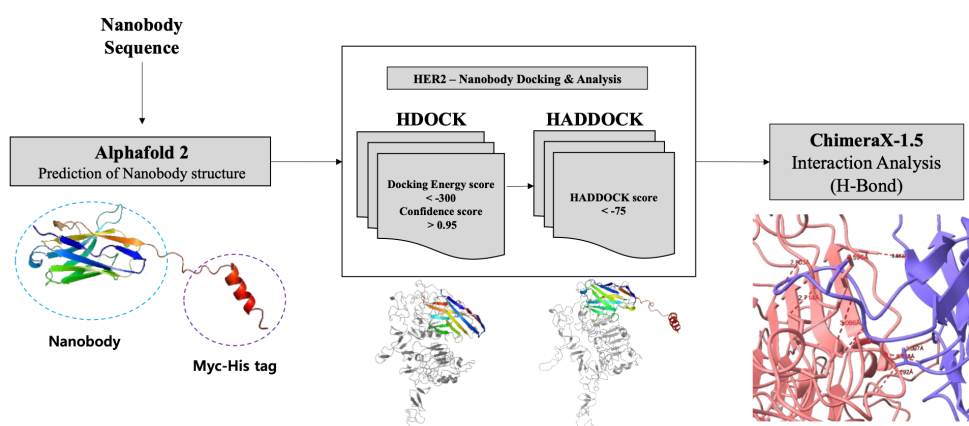
F



G

Ramachandran Plot (%)	Favored regions	Additional allowed regions	Generously allowed regions	Disallowed regions
OmegaFold	95.2	4.8	0.0	0.0
AlphaFold2	94.3	5.7	0.0	0.0
RosettaFold2	92.4	6.7	1.0	0.0
Nano-net	82.9	13.3	2.9	1.0

H



I

	Cell binding Rank	HDOCK Result	HADDOCK Result	Nanobody - HER2 H-Bond		Prediction binding site
				HDOCK	HADDOCK	
Nb51	1	Domain I	Domain I	9 bond	9 bond	Domain I
Nb16	3	Domain II	Domain II	3 bond	10 bond	Domain II
Nb49	4	Domain I	Fail to meet the condition	9 bond	-	Unknown
2Rs15d	-	Domain I	Domain I	15 bond	12bond	Domain I

Figure 5. Distinguish of nanobodies binding domain using *in-vitro* and *in-silico*. (A) The epitope binning result of each nanobody and trastuzumab using BLI. (B) The illustration of ELISA with MBP-fusion protein. (C) The SDS-PAGE-gel staining result of each MBP-fusion domains and BSA. (D) The result of fold change compared to negative control (MBP). The Nb51 concentration is 1 µg/ml, the Nb16 and Nb49 are 10 µg/ml. 20 ng/ml of trastuzumab was used for positive control. (E) Superimposing predicted models using OmegFold, AlphaFold2, RosettaFold2, Nano-Net. (F) ERRAT score of each server. (G) Residues rate chart of ramachandran plot results. (H) The schematic diagram of *in-silico* docking prediction. (I) Result of docking score of each HDOCK, HADDOCK and number of hydrogen bond by Chimera X.

5. Design of multi-paratopic nanobody using *in-silico*

Given the critical importance of HER2 domain II in conformation, we conducted a detailed structural analysis of HER2. Initially, we created a triangle using two residues (613, 619) parallel to the cell membrane and the highest residue (201) in domain I. Subsequently, we measured their heights using the Pymol program (Fig. 6A), revealing a difference of 5 angstroms and indicating a conformational change in domain II. To zoom in on domain II, we examined six HER2 structures, with three in the active form and the others in the endocytosis form. In domain II, the active forms exhibited higher heights than the endocytosis forms (Fig. 6B). This observation guided us in designing a multi-binding nanobody aimed at bending the conformation of domain II, thereby expect to induce an overall structural change (Fig. 6E). To further refine our approach, we analyzed the solvent-accessible surface area (SASA) of the HER2 structure, identifying candidate binding epitopes where the SASA % was over 60% in each domain (Fig. 6C). In domain I, we selected residues (122-131, 189-198) and negative residues (145-154) with SASA % under 10%. In domain II, residues (270-279, 333-341) were chosen and negative residues (239-247). In domain III, we selected residues (348-354, 382-390) and negative residues (464-470). These candidate epitope ranges were subjected to docking with nanobodies using HADDOCK (Fig. 6D). We selected docking models with the lowest docking score because it means binding energy. Following these steps, we identified the most likely binding epitopes for superimposition and calculated the distance from the N-terminal to the C-terminal of each nanobody (Fig. 6F). To facilitate the assembly of multiple nanobodies, considering (G₄S)₃ distance is 5.7 nm, we opted for flexible linkers (G₄S)₁, (G₄S)₃.

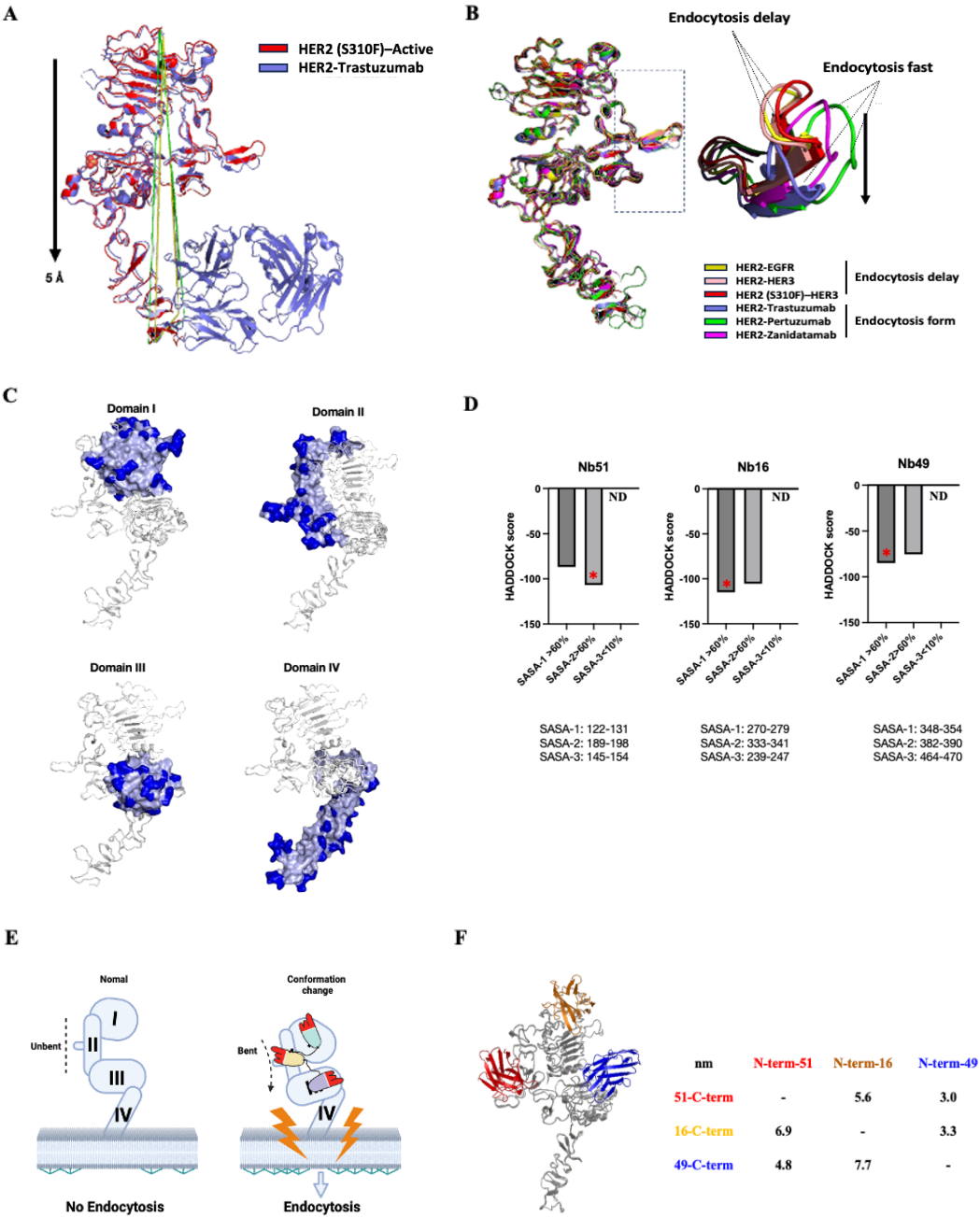


Figure 6. *In-silico* analysis of HER2 structures and design of multi-paratopic nanobody. (A) Comparison of height of HER2-S310F (PDB: 7MN6), HER2-Trastuzumab (PDB: 1N8Z). (B) Comparison of conformational changes of activation form (PDB: 7MN6, 8HGO, 7MN5) vs endocytosis form (PDB: 1N8Z, 1S78, 8FFJ) at domain II dimerization arm. (C) Analysis of HER2 (PDB: 6J71) solvent accessible surface area (SASA) (D) Candidate binding epitopes that has over SASA 60% were specified to compare docking score by HADDOCK. (E) Graphical abstract of multi-paratopic nanobody. (F) Superimposed docking model and distance of each nanobodies.

6. Effect of multi-paratopic nanobody

The multi-paratopic nanobodies were expressed in HEK 293T cells and purified using His resin. The SDS-PAGE gel results revealed that under reducing conditions, all nanobodies were expressed as anticipated (Fig. 7A). For validation of binding affinity, K_D values were measured through BLI, and a cell binding assay was conducted (Fig. 7B, C). In HER2-positive cell lines, all nanobodies exhibited binding to HER2, but in low HER2-expressing cells, their binding capability was diminished. Confocal imaging at high HER2 levels confirmed the binding of all nanobodies to HER2 (Fig. 7D). To assess the functional impact of each multi-paratopic nanobody, cell viability assays were performed in the NCI-N87 and SNU-1 cell lines (Fig. 7E). Trastuzumab served as the positive control, and all antibody concentrations were standardized as molar concentrations (nM). The 51-49-16 (G_4S)₁ exhibited an effect in NCI-N87. Furthermore, to investigate the endocytosis of multi-paratopic nanobodies, they were conjugated with a pH-sensitive dye and treated in NCI-N87 and SNU-1 cells (Fig. 7F). Trastuzumab conjugated with a pH-sensitive dye served as the positive control. Endocytosis fold change was high at 24 hours and 51-49-16 (G_4S)₁ showed faster endocytosis at 6 hours than any other multi-paratopic nanobodies at NCI-N87, although all of them exhibited a little endocytosis in SNU-1.

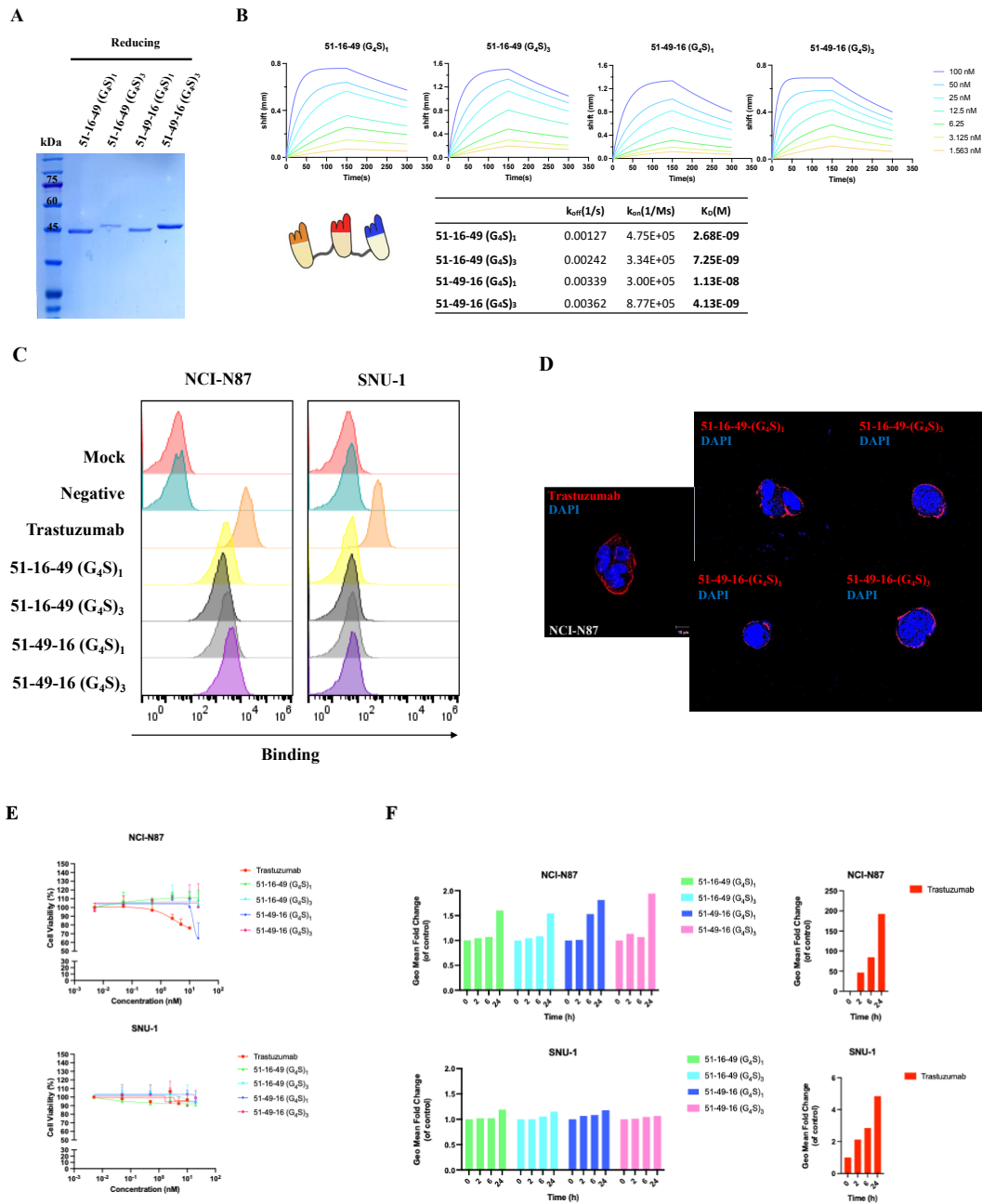
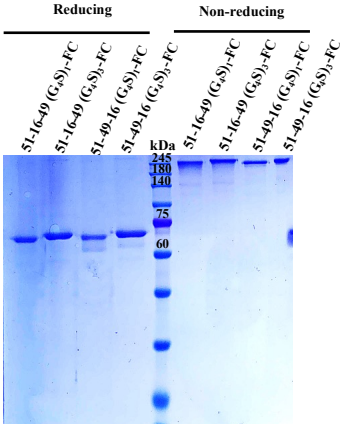


Figure 7. Purification and function of multi-paratopic nanobody. (A) SDS-PAGE gel image of purified multi-paratopic nanobody. (G₄S)₁ linker: 43.7 kDa, (G₄S)₃ linker: 44.9 kDa, (B) Binding affinity of multi-paratopic nanobody through BLI. (C) Measurement of cell binding assay in NCI-N87 (HER2 high) and SNU-1 (HER2 low). (D) Confocal image of each multi-paratopic nanobody binding HER2 at NCI-N87. (E) Cell viability of each multi-paratopic nanobody treated for 72 hr. (F) Measurement of endocytosis in multi-paratopic nanobody.

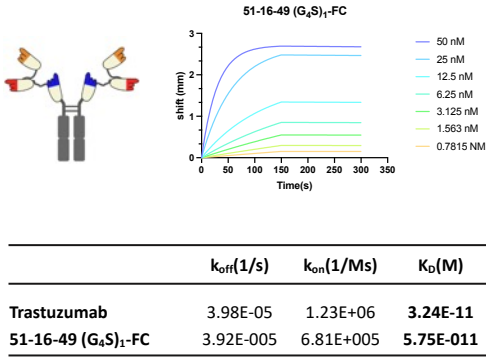
7. Effect of FC-fusion multi-paratopic nanobody

To assess whether the multimer effect increases upon forming a dimer, we generated Fc-fusion nanobodies in HEK293T and purified them with protein A beads. We confirmed their correct molecular weight through SDS-PAGE gel analysis (Fig. 8A). Additionally, the binding affinity of 51-16-49 (G₄S)₁-FC was measured using BLI, and it was found to be similar to the trastuzumab result (Fig. 8B). For the evaluation of cell binding, we utilized the NCI-N87 and SNU-1 cell lines. All of them exhibited similar binding affinity and confocal image results in NCI-N87, but none of them bound to SNU-1 (Fig. 8C, D). Lastly, we treated these constructs with NCI-N87 and SNU-1 to assess cell viability over 72 hours, and only 51-16-49 (G₄S)₁-FC demonstrated an effect in NCI-N87 (Fig. 8E).

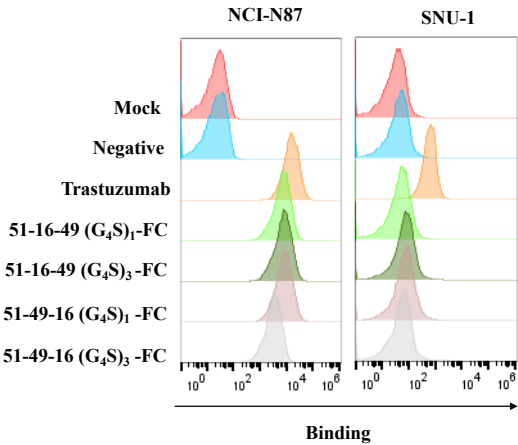
A



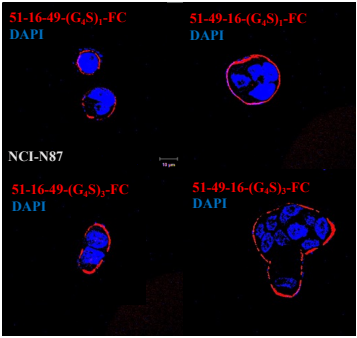
B



C



D



E

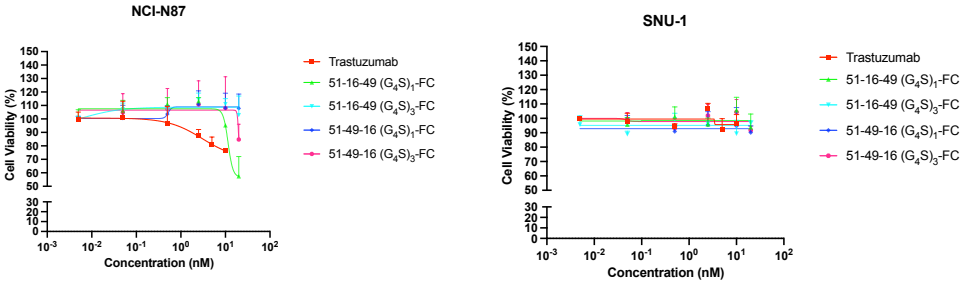


Figure 8. Purification and function of FC-fusion multi-paratopic nanobody. (A) SDS-PAGE gel image of purified multi-paratopic nanobody. (G₄S)₁ linker-FC fusion: 135 kDa, (G₄S)₃ linker-FC fusion: 137.4 kDa. (B) Binding affinity of 51-16-49 (G₄S)₁-FC, Trastuzumab through BLI. (C) Cell binding assay of each FC fusion multi-paratopic nanobody in NCI-N87 and SNU-1. (D) Confocal image of each FC-fusion multi-paratopic nanobody binding HER2 at NCI-N87. (E) Cell viability of each FC-fusion multi-paratopic nanobody treated for 72 hr.

IV. DISCUSSION

Gastric cancer (GC) remains a significant challenge in the field of oncology, primarily due to its high incidence and the associated healthcare burden. Within the context of GC, the overexpression of human epidermal growth factor receptor 2 (HER2) has garnered considerable attention, as it is prevalent in a substantial number of cases, similar to its role in breast cancer. The identification of HER2 as a crucial biomarker has paved the way for novel diagnostic and therapeutic strategies aimed at more effectively managing gastric cancer. However, it is important to note that unlike breast cancer, where HER2 overexpression is more common, the majority of gastric cancer cases exhibit low HER2 expression. This suggests that the efficacy of the current immunotherapeutic drug, Trastuzumab, is limited in most gastric cancer patients. This limitation was also observed in the case of T-DM1, a drug conjugate, where its effectiveness was found to be directly proportional to the level of HER2 expression (Fig. 1). Another point to note is the form of HER2 domain II. Unlike other family receptors, when heterodimer is formed with other receptors while maintaining an unbended form, intracellular cytopenia is delayed and sub-signals are produced constantly. The important point here is cytopenia, which is essential for intracellular drug delivery. Therefore, improving drug delivery in low HER2 expression requires the production of multiple paratopic antibodies to influence single HER2 domain II structures while inducing overall structural morphological changes. Our study leveraged advanced techniques such as ribosome display, phage display, and ELISA to identify nanobodies capable of specifically targeting HER2 (Fig. 3A). Notably the selection of nanobody Nb51, which exhibited the highest binding affinity among the candidates (Fig. 3D). One of the key contributions of our research is the discovery of nanobodies that selectively bind to different domains of the HER2 receptor by using *in-vitro* and *in-silico* methods. Nb51, Nb16, and Nb49 target distinct domains of HER2, while Trastuzumab serves as a positive control, binding to Domain IV (Fig. 5B). Importantly, our results confirm that these nanobodies do not interfere with each other's binding, suggesting the feasibility of combining them for tailored therapies. This

distinction of binding domains adds a new dimension to HER2-targeted treatment strategies in gastric cancer. In *in-silico*, the structural analysis of HER2, particularly the conformational changes observed in Domain II, guided our efforts to design a multi-binding nanobody (Fig. 6A, B). By identifying candidate binding epitopes and incorporating flexible linkers, our goal was to induce structural changes in HER2, potentially enhancing endocytosis. Unfortunately, while we achieved improved binding affinity over single nanobodies (Table 2), we only observed cell binding affinity in NCI-N87 cells highly expressing HER2 (Fig. 7). Moreover, as it did not bind in SNU-1 cells expressing low HER2, it is considered to selectively bind to cells with elevated HER2 expression, despite our initial design to target a single HER2. Notably, 51-49-16 (G₄S)₁, which exhibited a low K_D value among multimers, demonstrated an effect on cell viability and confirmed faster intracellular uptake compared to other nanobodies in terms of endocytosis. This suggests that the order of binding may play a crucial role. We recently demonstrated that an anti-HER2 DARPIn dimer targeting domains I-IV induces HER2 inactivation conformation²⁷. Therefore, it appears that 51-49 is exhibiting a similar effect as it binds to domain I-III. Furthermore, in the case of Fc-fusion (Fig. 8), 51-16-49 (G₄S)₁-FC showed an effect, and it remains unknown how the strong binding force of the two components may have altered HER2. To confirm this, crystal structure photography should be conducted. Additionally, to elucidate endocytosis by the bending structure at low HER2 expression levels, it is advisable to increase the binding affinity of each nanobody. As we advance, ongoing research will be crucial to validate the utility of these nanobodies and realize their potential in improving outcomes for patients with gastric cancer. The iterative refinement and optimization of these nanobodies based on both experimental and computational approaches will contribute to the development of more effective and targeted therapeutic strategies HER2 in malignant tumors such as gastric cancer and potentially other related malignancies.

V. CONCLUSION

In this study, we initially identified numerous nanobodies that bind to HER2, distinguishing three nanobodies with distinct binding sites through in-silico methods and *in-vitro* experiments. Subsequently, we generated multi-paratopic nanobodies designed from HER2 structure analysis using in-silico methods. Specifically, we measured the distance of each nanobody from docking models predicted in-silico and used flexible linkers of varying lengths to induce a bending structure in HER2, producing multi-paratopic nanobodies. Although each nanobody exhibited low binding affinity, we confirmed an enhancement in binding affinity by generating multimers. In cell binding, viability results, and intracellular uptake assays, these nanobodies demonstrated efficacy only in cells with high HER2 expression. Particularly, 51-49-16 (G₄S)₁, despite its lower binding affinity compared to other multi-paratopic nanobodies, showed effectiveness in cell viability and exhibited intracellular uptake within 6 hours. As a result, our research proposes the design of multi-paratopic nanobody applying in-silico methods to induce HER2 inactivated by structural changes in itself for HER2 in malignant tumors such as gastric cancer.

REFERENCES

1. H. Sung, J. Ferlay, R. L. Siegel, M. Laversanne, I. Soerjomataram, A. Jemal, et al. "Global cancer statistics 2020: GLOBOCAN estimates of incidence and mortality worldwide for 36 cancers in 185 countries." *CA: a cancer journal for clinicians* 71.3 (2021): 209-249
2. Gravalos, Cristina, and Antonio Jimeno. "HER2 in gastric cancer: a new prognostic factor and a novel therapeutic target." *Annals of oncology* 19.9 (2008): 1523-1529.
3. I. Rajagopal, S. Niveditha, R. Sahadev, P. K. Nagappa and S. G. Rajendra. "HER2 expression in gastric and gastro-esophageal junction (GEJ) adenocarcinomas" *Journal of clinical and diagnostic research: JCDR* 9.3 (2015): EC06.
4. Y.-J. Bang, E. Van Cutsem, A. Feyereislova, H. C. Chung, L. Shen, A. Sawaki, et al. "Trastuzumab in combination with chemotherapy versus chemotherapy alone for treatment of HER2-positive advanced gastric or gastro-oesophageal junction cancer (ToGA): a phase 3, open-label, randomised controlled trial." *The Lancet* 376.9742 (2010): 687-697.
5. R. V. Kholodenko, D. V. Kalinovsky, I. I. Doronin, E. D. Ponomarev and I. V. Kholodenko. "Antibody fragments as potential biopharmaceuticals for cancer therapy: success and limitations." *Current Medicinal Chemistry* 26.3 (2019): 396-426.
6. F. M. Yakes, W. Chinratanalab, C. A. Ritter, W. King, S. Seelig and C. L. Arteaga. "Herceptin-induced inhibition of phosphatidylinositol-3 kinase and Akt Is required for antibody-mediated effects on p27, cyclin D1, and antitumor action." *Cancer research* 62.14 (2002): 4132-4141.

7. Kono K, Takahashi A, Ichihara F, Sugai H, Fujii H, Matsumoto Y. Impaired antibody-dependent cellular cytotoxicity mediated by herceptin in patients with gastric cancer. *Cancer Res.* 2002 Oct 15;62(20):5813-7
8. L. N. Klapper, H. Waterman, M. Sela and Y. Yarden. "Tumor-inhibitory antibodies to HER-2/ErbB-2 may act by recruiting c-Cbl and enhancing ubiquitination of HER-2." *Cancer research* 60.13 (2000): 3384-3388.
9. P. M. Pereira, S. K. Sharma, L. M. Carter, K. J. Edwards, J. Pourat, A. Ragupathi, et al. Caveolin-1 mediates cellular distribution of HER2 and affects trastuzumab binding and therapeutic efficacy. *Nat Commun* 9, 5137 (2018).
10. T. Yang, R. Xu, J. You, F. Li, B. Yan and J.-n. Cheng. Prognostic and clinical significance of HER-2 low expression in early-stage gastric cancer. *BMC Cancer* 22, 1168 (2022).
11. Bouchard, Hervé, Christian Viskov, and Carlos Garcia-Echeverria. "Antibody–drug conjugates—a new wave of cancer drugs." *Bioorganic & medicinal chemistry letters* 24.23 (2014): 5357-5363.
12. M. Yu, Y. Liang, L. Li, L. Zhao and F. Kong. "Research progress of antibody-drug conjugates therapy for HER2-low expressing gastric cancer." *Translational Oncology* 29 (2023): 101624.
13. J. Cheng, M. Liang, M. F. Carvalho, N. Tigue, R. Faggioni, L. K. Roskos, et al. "Molecular mechanism of HER2 rapid internalization and redirected trafficking induced by anti-HER2 biparatopic antibody." *Antibodies* 9.3 (2020): 49.
14. T. Komatsu, E. Kyo, H. Ishii, K. Tsuchikama, A. Yamaguchi, T. Ueno, et al. "Antibody clicking as a strategy to modify antibody functionalities on the surface of

- targeted cells." *Journal of the American Chemical Society* 142.37 (2020): 15644-15648.
15. F. Kast, M. Schwill, J. C. Stüber, S. Pfundstein, G. Nagy-Davidescu, J. M. M. Rodríguez, et al. Engineering an anti-HER2 biparatopic antibody with a multimodal mechanism of action. *Nat Commun* **12**, 3790 (2021).
 16. Y. Yan, X. Cheng, L. Li, R. Zhang, Y. Zhu, Z. Wu, et al. "A novel small molecular antibody, HER2-nanobody, inhibits tumor proliferation in HER2-positive breast cancer cells in vitro and in vivo." *Frontiers in Oncology* 11 (2021): 669393.
 17. D. Ubbiali, M. Orlando, M. Kovačič, C. Iacobucci, M. S. Semrau, G. Bajc, et al. "An anti-HER2 nanobody binds to its antigen HER2 via two independent paratopes." *International journal of biological macromolecules* 182 (2021): 502-511.
 18. I. Zimmermann, P. Egloff, C. A. Hutter, F. M. Arnold, P. Stohler, N. Bocquet, et al. Synthetic single domain antibodies for the conformational trapping of membrane proteins. *eLife* **7**, e34317 (2018).
 19. J. B. Hughes, C. Berger, M. S. Rødland, M. Hasmann, E. Stang and I. H. Madhus. "Pertuzumab increases epidermal growth factor receptor down-regulation by counteracting epidermal growth factor receptor-ErbB2 heterodimerization." *Molecular cancer therapeutics* 8.7 (2009): 1885-1892.
 20. X. Bai, P. Sun, X. Wang, C. Long, S. Liao, S. Dang, et al. "Structure and dynamics of the EGFR/HER2 heterodimer." *Cell Discovery* 9.1 (2023): 18.
 21. D. Diwanji, R. Trenker, T. M. Thaker, F. Wang, D. A. Agard, K. A. Verba, et al. "Structures of the HER2–HER3–NRG1 β complex reveal a dynamic dimer interface." *Nature* 600.7888 (2021): 339-343.
 22. H. Yu, G. Mao, Z. Pei, J. Cen, W. Meng, Y. Wang, et al. "In Vitro Affinity Maturation of Nanobodies against Mpox Virus A29 Protein Based on Computer-Aided Design"

Molecules 2023 Vol. 28 Issue 19 Pages 6838

23. M. A. Soler, S. Fortuna, A. De Marco and A. Laio. "Binding affinity prediction of nanobody–protein complexes by scoring of molecular dynamics trajectories" *Physical Chemistry Chemical Physics* 2018 Vol. 20 Issue 5 Pages 3438-3444
24. X. Zeng, G. Bai, C. Sun and B. Ma. "Recent Progress in Antibody Epitope Prediction." *Antibodies* 2023 Vol. 12 Issue 3 Pages 52
25. G. Van Zundert, J. Rodrigues, M. Trellet, C. Schmitz, P. Kastiris, E. Karaca, et al. "The HADDOCK2. 2 web server: user-friendly integrative modeling of biomolecular complexes" *Journal of molecular biology* 2016 Vol. 428 Issue 4 Pages 720-725
26. Y. Yan, H. Tao, J. He and S.-Y. Huang. "The HDock server for integrated protein–protein docking" *Nature protocols* 2020 Vol. 15 Issue 5 Pages 1829-1852
27. J. C. Stüber, C. P. Richter, J. S. Bellón, M. Schwill, I. König, B. Schuler, et al. "Apoptosis-inducing anti-HER2 agents operate through oligomerization-induced receptor immobilization" *Communications Biology* 2021 Vol. 4 Issue 1 Pages 762

APPENDICES

Table 1. Result of docking scores (A) Result of HDock docking score. (B) Result of HADDOCK score. Postive control is 2Rs15d structure (PDB: 5MY6).

A					B				
HDock score	Target range				HADDOCK score	Target range			
	I	II	III	IV		I	II	III	IV
Nb51	-577.92	-577.74	-296.81	-293.07	Nb51	-89.6 +/- 3.3	-53.1 +/- 4.2	-63.6 +/- 10.1	98.5 +/- 20.0
Nb55	-620.14	-619.81	-287.17	-283.74	Nb55	-79.2 +/- 6.9	-13.8 +/- 5.6	-58.3 +/- 5.8	109.7 +/- 10.9
Nb16	-341.74	-343.87	-338.48	-266.23	Nb16	58.0 +/- 8.4	-147.3 +/- 2.9	-45.3 +/- 7.2	106.7 +/- 10.1
Nb49	-305.34	-304.65	-288.15	-281.79	Nb49	-64.9 +/- 7.2	-15.5 +/- 6.5	-42.5 +/- 7.8	104.3 +/- 9.7
Nb11	-336.55	-338.84	-265.1	-265.32	Nb11	-112.6 +/- 4.4	25.6 +/- 8.6	-33.6 +/- 3.8	42.5 +/- 6.6
Nb2	-408.89	-408.98	-317.04	-317.13	Nb2	-92.7 +/- 7.8	3.9 +/- 11.8	-112.1 +/- 5.7	114.0 +/- 3.2
Nb56	-311.93	-313.04	-271.37	-271.37	Nb56	33.4 +/- 4.5	-149.1 +/- 8.4	22.8 +/- 6.5	81.2 +/- 8.3
Nb58	-576.89	-576.72	-286.12	-256.05	Nb58	-88.8 +/- 3.3	-27.9 +/- 13.8	-28.6 +/- 4.2	87.2 +/- 10.9
Nb27	-348.5	-348.36	-281.08	-280.84	Nb27	-80.0 +/- 4.5	-18.1 +/- 6.9	-21.5 +/- 14.9	101.8 +/- 18.1
2Rs15d	-307.39	-268.7	-237.72	-235.97	2Rs15d	-93.7 +/- 1.4	-43.2 +/- 3.8	-35.6 +/- 3.7	107.7 +/- 4.0

Table 2. Result of binding affinity

	$k_{off}(1/s)$	$k_{on}(1/Ms)$	$K_D(M)$
Trastuzumab	3.98E-05	1.23E+06	3.24E-11
Nb51	1.06E-01	1.78E+05	5.97E-07
Nb16	9.62E-03	4.97E+04	1.93E-07
Nb49	4.07E-02	3.05E+04	1.33E-06
51-16-49 (G4S) ₁	1.27E-03	4.75E+05	2.68E-09
51-16-49 (G4S) ₃	2.42E-03	3.34E+05	7.25E-09
51-49-16 (G4S) ₁	3.39E-03	3.00E+05	1.13E-08
51-49-16 (G4S) ₃	3.62E-03	8.77E+05	4.13E-09
51-16-49 (G4S) ₁ -FC	3.92E-005	6.81E+005	5.75E-011

ABSTRACT (IN KOREAN)

HER2 불활성화 굽힘구조를 유도하는 항-HER2 다중결합 나노바디 설계

<지도교수 김 주 영>

연세대학교 대학원 의과학과

김 도 현

트라스투주맵(Trastuzumab)은 HER2 수용체를 특이적으로 표적하는 단일 클론 항체로, 세포 성장을 억제하고 세포 사멸을 유도하는 데 효과적으로 사용되고 있습니다. 더불어, 트라스투주맵을 이용한 T-DM1은 약물을 세포 내로 효과적으로 전달하면서 세포 사멸을 촉진합니다. 그러나 HER2 발현이 낮은 암 세포에서는 이 효과가 제한될 수 있습니다. 최근 연구에서는 HER2의 도메인 II 부분이 이종이량체 (Heterodimer) 세포 내 유입을 억제하는 역할을 한다고 보고되었습니다. 본 연구에서는 HER2의 여러 도메인과 결합하는 나노바디들을 발굴하여 향상된 결합력을 가질 뿐 아니라 HER2 도메인 II의 구조적 변화를 통해 불활성화를 유도하는 다중 파라토프 나노바디를 설계했습니다. 10^{12} 다양성을 가진 합성 나노바디 라이브러리의 스크리닝을 통해 여러 개의 나노바디를 발견한 후 *in silico* 방법으로 HER2에 결합하는 부위를 예측하고, 실제 조각난 HER2단백에 결합함을 생화학적인 방법으로 확인하여 각기 다른 도메인 I, II, 및 III 부위에 결합하는 나노바디들을 선정하였습니다. 3개를 다른 순서로 연결한 다중결합 형태 중, I, III, II 순서로 짧은 유연링커로 붙은 형태가 효과가 있었고 이들의 Fc 형태에서는 I, III, II 순서보다 결합력이 높은 I, II, III 순서가 효과가 있음을 확인하였습니다. 결론적으로 본 연구는 위암과 같은 악성 종양에서 HER2에 대한 결합친화도를 증가하는 것뿐 아니라 HER2 자체의 구조적인 변화를 유도하여 HER2에 대한 새로운 불활성화 전략을 제공합니다.

핵심되는 말 : HER2, 다중결합, 세포내이입, 나노바디, 트라스투주맙, 인실리코 방법